

# Optimising EV Efficiency with Hybrid Energy Storage and Advanced Control Strategies

Mostafa Farrag

Brunel University London  
Department of Electronic and Electrical  
Engineering, London, UK  
[mostafa.farrag@brunel.ac.uk](mailto:mostafa.farrag@brunel.ac.uk)

Chun Sing Lai

Brunel University London  
Department of Electronic and Electrical  
Engineering, London, UK  
[chunsing.lai@brunel.ac.uk](mailto:chunsing.lai@brunel.ac.uk)

Mohamed Darwish

Brunel University London  
Department of Electronic and Electrical  
Engineering, London, UK  
[mohamed.darwish@brunel.ac.uk](mailto:mohamed.darwish@brunel.ac.uk)

**Abstract**—This study examines a hybrid energy storage system (HESS) that integrates Lithium-Ion Batteries (LIB) with Supercapacitors (SCs). The HESS is built with a completely active topology that guarantees precise regulation of energy flow. Comparison of Proportional-Integral (PI) and Online Radial Basis Function (RBF) controllers is conducted via simulations are performed utilising representative driving cycles. The Online RBF controller surpasses the PI controller by reducing power losses and ensuring stable State of Charge (SoC) profiles. The results emphasise how HESS can improve Electric Vehicle (EV) performance and emphasise the vital role of control methods in attaining optimal energy management.

**Keywords**— *Electric vehicle, hybrid energy storage system; battery; supercapacitor; performance; simulation.*

## I. INTRODUCTION & RELATED WORK

As EVs continue to gain prominence in the automotive landscape, the efficacy of their propulsion systems hinges significantly upon the capabilities of the Energy Storage System (ESS). At the forefront of ESS technologies, the LIB has emerged as a prevalent choice because of its high energy density. Despite its widespread use, the LIB has drawbacks such as low power density, limited cycle life and being the most expensive component of an EV [1][2]. Addressing these nuanced aspects becomes paramount for furthering the evolution of electric propulsion systems in terms of efficiency, sustainability, and economic viability.

To address the issue of reducing stress on the battery under different circumstances of driving, supercapacitors (SCs) is integrated to create a hybrid energy storage system (HESS). SCs are high-power-density energy stores with greater cycle life in comparison with LIB's. SCs are capable of absorbing the substantial dynamic traction power demand, thus reducing battery ageing stress [3]. E.g. When a vehicle is moving up a hill, the supercapacitor can deliver a large amount of power rapidly, and during downhill it can recharge the supercapacitor [4].

The essential challenge in the design of a HESS for EV is to manage the current flow between the supercapacitors and the battery. The merits and demerits of various topologies of HESS have been comprehensively reviewed in the existing academic literature [4][5][6]. As well known the use of a bidirectional DC-DC converter is crucial in a HESS design, where it combines batteries and supercapacitors, where it for energy to flow in both directions between the two energy storage elements. HESS systems are designed to take benefit of the complementary characteristics of batteries and supercapacitors to optimise energy storage and delivery. For this proposed work, the fully active topology used in HESS is distinguished by its ability to precisely manage energy

flow, resulting in optimal operational performance. This approach enhances energy efficiency through the strategic utilisation of diverse storage technologies, ensuring an adaptive and dynamic response to fluctuating load demands.

In Ref [7], polynomial control was utilised to handle the power for two DC-DC converters, and the results were similar to the traditional PI. The latest research adopted rules-based techniques such as fuzzy logic control for regulating HESS power distribution [8]. Additionally, recent research has concentrated on rule-based techniques, such as fuzzy logic control, in order to regulate the flow of power in the HESS [8]. An energy management approach was implemented based on the adaption of fuzzy logic and the reliability of monitoring uncertainty. The feature of membership and fuzzy rule, on the other hand, were both designed with human experience in consideration. Consequently, it won't be capable of maintaining adequate control performance in unanticipated scenarios. A comparison was carried out between the performance of a non-linear model predictive controller, a linear model predictive controller, and rule-based control in Ref [9]. The study was performed on an EV energy storage system comprised of a combination of battery and supercapacitor. Another study has examined fuzzy controllers to rule-based HESS regulators to lengthen the battery lifespan. The findings reveal that amid fluctuations the controllers draw power directly from the supercapacitor to supply the EV load current, whereas during steady state, the battery became the source of the load current [10]. The researchers used multi-objective optimisation to extend the driving cycle and reduce the bulk of HESS in Ref [11]. The suggested regulator was validated using three common drive cycles.

Developing a control procedure for HESS for an electric vehicle is the ultimate goal of this paper. Two control techniques, namely online radial basis function (RBF) and proportional-integral (PI) controllers, have been selected, due to their lower computational complexity, ease of real-time implementation and robust performance in scenarios with well-understood system dynamics. Four sections make up this paper. The second section presents a discussion on system modelling. In the third section, the outcomes of the simulations are laid out, and in the fourth section, the findings are stated.

## II. SUMMARY OF THE SYSTEM AND MODELLING

### A. Organisational Framework

Connecting the SC and battery pack power sources to the driving system is accomplished through the utilisation of a DC-DC converter [12]. To ensure that the system is charged and discharged with great efficiency, power converters that are equipped with an ESS are required to regulate the

distribution of power bidirectionally [12]. As depicted in Figure 1, the architecture of the examined HESS was thus constructed utilising fully active topology. With this setup, the sources can receive power demands with a high degree of precision. Additionally, it provides excellent durability and adaptability in how it operates, with a consistent current flow that is advantageous for handling voltage fluctuations. However, it is characterised by sophisticated regulation and a greater amount of semiconductor switches [13].

Figure 1 demonstrates that by utilising parallel converters, it feasible to allow a negative power flow exclusively in the SCs, where from its recognised for its substantial charge and discharge capabilities. For SC system, buck-boost converter is employed, connected to the SC to serve the dual purpose of discharging as a boost converter and charging as a buck converter. The adoption of a buck-boost converter for the SC ensures efficient energy transfer during both charging and discharging phases, allowing for versatile operation and effective utilisation of the SC's high charge and discharge capacities. The adoption of boost converter for battery, only taking part on the discharge.

The controllers play a crucial role in regulating and managing the power flow within the system. In this study, a comparative analysis between PI and online RBF controllers is conducted. This choice is driven by the well-established mathematical frameworks associated with PI and Online RBF, which provide a foundation for precise and robust control. The comparison is particularly relevant in the context of regulating the fully active topology of the HESS. Subsequently, detailed explanations of the PI and Online RBF controllers will be provided to illuminate their specific contributions and applications within the system.

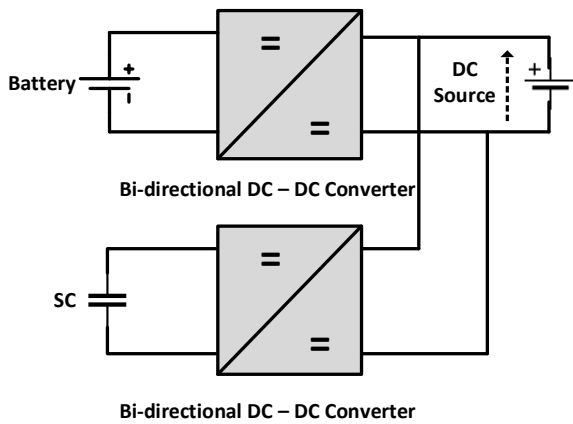


Figure 1. Fully Active HESS Topology

### B. Vehicle Model

Developing a reliable model of an EV's behaviour is the initial stage in studying and enhancing the efficiency of the EV's power consumption. Figure 2 depicts the forces acting on the EV's movement, which are the primary dynamics. These forces are the aerodynamic force, the rolling force, the acceleration force, and the grading force. Equation 1 can be used to determine total force.

$$F_{Total} = F_{aero} + F_{roll} + F_{grad} + F_{accel} \quad (1)$$

The variables  $F_{aero}$ ,  $F_{roll}$ ,  $F_{grad}$ ,  $F_{grad}$ , and  $F_{accel}$  denote the forcing components of aerodynamic, rolling resistance, gravitational force, and acceleration, respectively.

As the vehicle travels, it encounters forces acting against it, one of which is the aerodynamic force, which arises from the interaction of incoming and outgoing air while the vehicle is on the move. The vehicle front sections, front bulges such as side mirrors and air gaps can contribute to the opposing force that is being exerted [14]. The aerodynamic force can be determined by using Equation 2.

$$F_{aero} = 0.5 \rho C_d A_f v^2 \quad (2)$$

The variables in the equation are air density ( $\rho$ ), drag coefficient ( $C_d$ ), area of the front part of the vehicle ( $A_f$ ), and speed of the vehicle ( $v$ ). The primary source of rolling resistance is the frictional among the road surface and the tyre. Ball bearing friction and the power transmission system both contribute to the rolling resistance. The rolling resistance is directly proportional to the vehicle's mass. Equation 3 demonstrates horizontal road rolling resistance force [14].

$$F_{roll} = C_{rr} m g \cos (\theta) \quad (3)$$

Where  $C_{rr}$  represents the rolling resistance coefficient,  $m$  denotes the vehicle's mass in kilo grams, and  $g$  signifies the earth's gravitational acceleration in metres per second. Equations (4) and (5) are applied for determining the gravitational force, acceleration force, and passing gradient force, accordingly [14].

$$F_{grad} = m g \sin (\theta) \quad (4)$$

$$F_{accel} = m a \quad (5)$$

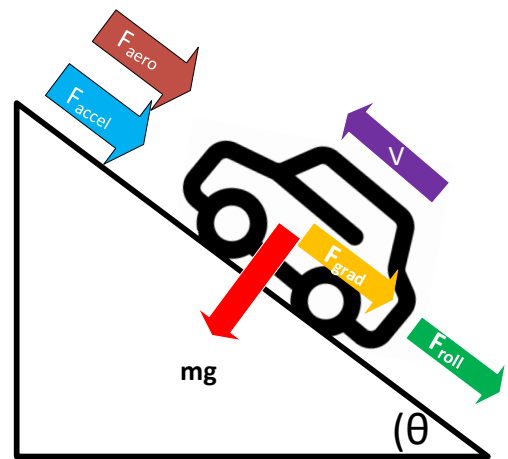


Figure 2 - Measurement of Vehicle Dynamics

### C. Battery Model

An equivalent circuit model is a widely used representation that utilise electrical elements to replicate the battery's activity. There are several ways to depict the electrical equivalent circuit model for the battery. Most of these representations can be categorised into three basic types, which are Thevenin, impedance, and runtime models [15].

A battery from the Simulink library of MATLAB/SIMULINK was utilised for simulation purposes in this paper. As illustrated in Figure 3, this equivalent model incorporates a control voltage source and an internal resistance. Equation 6 illustrates the association among the time-varying parameters within the battery model.

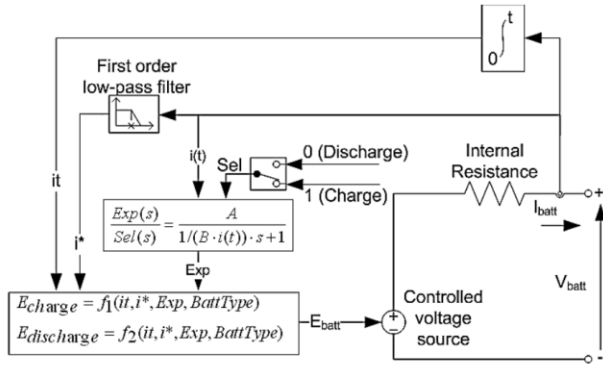


Figure 3. Equivalent Circuit of Battery in SIMULINK

#### D. Supercapacitor Model

Figure 3 illustrates the mathematical description and equivalent circuit of the SC, which was modelled in this study using the MATLAB/Simulink. By combining the theoretical knowledge given in Equation 6 with a realistic simulation environment, this approach allows for a thorough investigation of the supercapacitor's behaviour and features. Researchers can delve deeper into the SC system's dynamics thanks to the integrated equivalent circuit, mathematical model, and simulation platform [14].

$$V_{LSC} = V_{SC} - R_{SC} I_{SC} \quad (6)$$

Where the variables denoted as  $V_{LSC}$ ,  $V_{SC}$ ,  $R_{SC}$  and  $I_{SC}$ , respectively represents the terminal voltage of the SC, voltage of the SC, internal resistance and the current direction of the supercapacitor, positive for charging and negative for discharging.

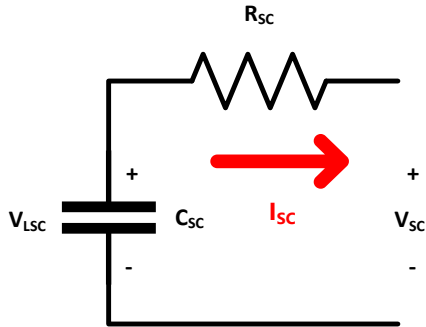


Figure 4. Equivalent Circuit of a SC

### III. CONTROLLER DESIGN

This section outlines the control methods used in designing a HESS for EVs, which combines a battery and SC. Two unique control methods, PI and Online RBF, are investigated.

Mathematical properties of PI controller and Online RBF controller in HESS DC-DC converters for the battery (connected to buck converter) and the Supercapacitor (connected to buck-boost converter) are examined.

#### A. PI Controller

The mathematical expressions for the PI controller characteristics regulating the behaviour of the battery, which is linked to the buck converter, and the SC, connected to the buck-boost converter, are outlined in Equations 7 & 8 [16].

For battery (Buck Converter)

$$U_{bat}(t) = K_{p_{bat}} e_{bat}(t) + K_{i_{bat}} \int_0^t e_{bat}(\tau) dt \quad (7)$$

For SC (Buck-Boost Converter)

$$U_{SC}(t) = K_{p_{SC}} e_{SC}(t) + K_{i_{SC}} \int_0^t e_{SC}(\tau) dT \quad (8)$$

Where:

$U_{bat}(t)$  and  $U_{SC}(t)$ : Control signals for the battery and SC

$K_{p_{bat}}$ ,  $K_{i_{bat}}$ ,  $K_{p_{SC}}$  and  $K_{i_{SC}}$ : Proportional and integral gains for the battery and SC controllers.

$e_{bat}(t)$  and  $e_{SC}(t)$ : Error signals for the battery and SC

#### B. Online RBF

Online RBF controller is characterised by its adaptability and ability to approximate complex, non-linear systems. It utilises radial basis functions as basis functions in its network. The output of the RBF controller can be expressed in Equation 9 [16].

$$u(t) = \sum_{j=1}^N w_j \phi_j(x(t)) \quad (9)$$

Where:

$w_j$ : Weights associated with each radial basis function

$\phi_j(x(t))$ : Radial basis function centred at  $x(t)$

$N$ : Total number of radial basis functions

Adaptive mechanisms are commonly utilised by online RBF to modify the weight based on system's current state, enabling it to adopt to varying conditions. This adaptability is particularly advantageous in HESS applications where the dynamics of energy storage and delivery can change rapidly [16].

### IV. SIMULATION FINDINGS AND ANALYSIS

MATLAB/Simulink is used for modelling an evolving model of an EV that has been proposed. This model includes LIB and a SC. The specifications of the dynamic model of the proposed vehicle that have been generated through simulation, LIB's and supercapacitors are illustrated in Table I.

The selection of driving cycles is important in analysing the operation of control methods for PI and online RBF controllers in HESS for EVs. Driving cycles represent realistic vehicle speed and power requirements across a period of time. Selecting two distinct drive cycles enables researchers to assess how the HESS performs under varying operational circumstances. These cycles can encompass situations such as urban commuting with frequent acceleration and deceleration or motorway. By analysing a wide range of driving scenarios, the suitability and efficiency of the selected control methods can be assessed thoroughly.

For simulation DC source has been used to compensate motor for HESS. Flowchart that can be seen in Figure 5 highlights the dynamic process in an EV mechanism. The battery provides power to meet average demand, while a DC source provides power to SC to aid during acceleration and stores energy during deceleration to the SC, facilitating persistent and optimised power delivery.

In the following part, an in-depth investigation of the functionality of both the PI and Online RBF controllers will focus on particular performance metrics, response characteristics, and efficiency improvements seen during each of the chosen driving cycles, which are US06 and SC03.

Table I. Simulation Module-Specific Parameters

Module	Parameter	Value
EV	$C_{rr}$	1
	$C_d$	1
	$m$	1567 kg
	$A_f$	1 m <sup>2</sup>
Battery	Nominal Voltage of the Cell	3.7 V
	Rated capacity	47 Ah
SC	Nominal Voltage	16 V
	Rated capacitance	500 F
	Number of series capacitors	6
	Number of parallel capacitors	1

### A. US06

The US06 driving cycle is widely utilised to evaluate the effectiveness of a HESS strategy for EVs in a variety of real-world scenarios. It includes an average speed of 77.9 km/h, 20 acceleration points, and five complete stops [14]. Speed driving cycle profile of US06 can be seen in Figure 6(a), from section 2 power demand profile can be calculated based on mathematical Equations (1 to 5). Power demand profile can be seen in Figure 6 (b). Outcomes results of US06 cycle are displayed in Figures 6 to 10, providing insight into the behaviour of the system under various environmental conditions.

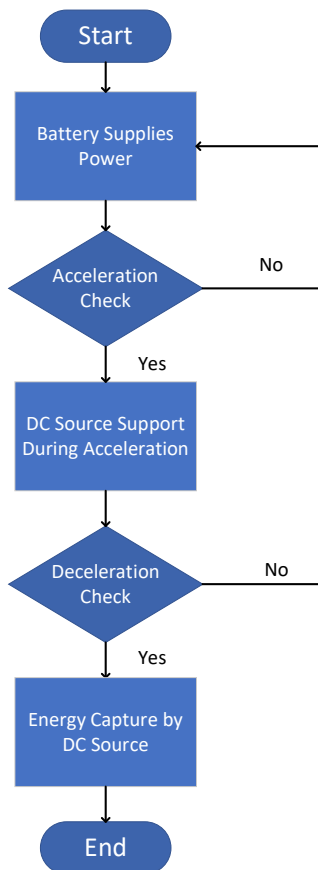


Figure 5. Flowchart of Operation of HESS

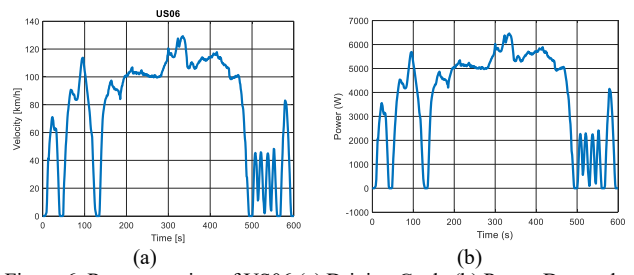


Figure 6. Representation of US06 (a) Driving Cycle (b) Power Demand

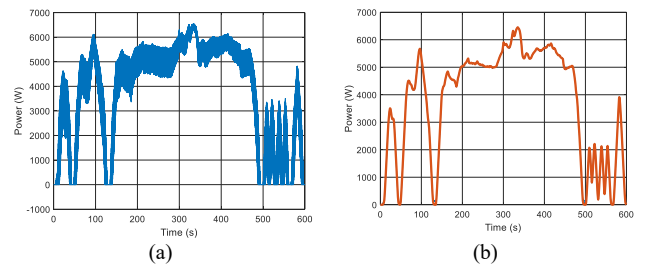


Figure 7. Representation of US06 Battery Profile for (a) PI Controller (b) Online RBF Controller

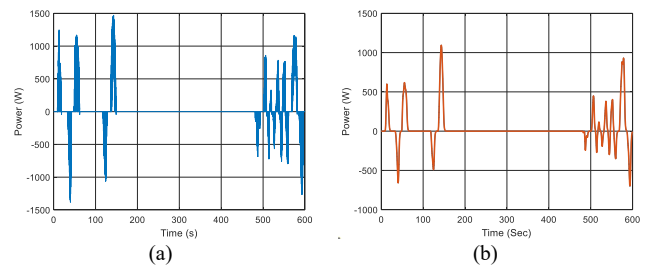


Figure 8. Representation of US06 SC Profile for (a) PI Controller (b) Online RBF Controller

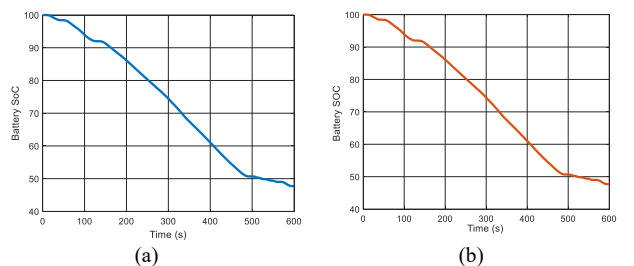


Figure 9. Representation of US06 Battery SoC Profile for (a) PI Controller (b) Online RBF Controller

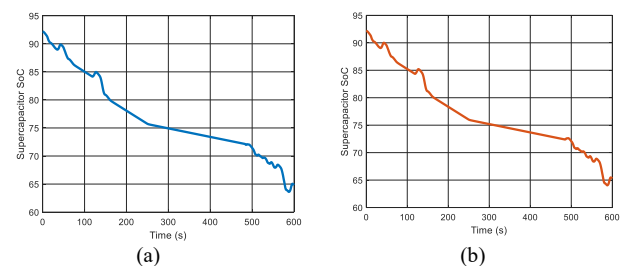


Figure 10. Representation of US06 SC SoC Profile for (a) PI Controller (b) Online RBF Controller

### B. SC03

The SC03 driving cycle is also another famous cycle that is widely used to evaluate the effectiveness of a HESS strategy for EVs in a variety of real-world scenarios. The average speed included in the SC03 driving cycle is 34.8 km/h a. With a total of 18 accelerations and 197 seconds of deceleration, the cycle comprises of 236 seconds of acceleration. Includes six stops, the average length of which is 13.67 seconds. Speed driving cycle and power demand profiles can be seen in Figure 11. Outcomes results of SC03

cycle are displayed in Figures 11 to 15, providing insight into the behaviour of the system under various environmental conditions.

### C. Discussion

The battery power profile maintains to provide a significant portion of the typical demand for power for both controllers of the vehicle, as illustrated in Figures 7 & 12. This is because the sole function of a DC source is to provide power to the battery while accelerating and to capture energy while decelerating. Even though both controllers provide a similar battery power profile, the online RBF controller demonstrates a steady power profile due to its capability of optimising control inputs in response to the current state of the system, whereas the PI controller exhibits significant power fluctuations.

The SC provides the required power fluctuations as shown in Figures 8 & 13 for both. It can be seen PI controller generates higher charge/discharge rate of SC, this tends to be responsiveness to instantaneous errors and its tendency to react quickly to changes in the system. Yet, this increased responsiveness could result in more strain on the SC, leading to greater variations in the charging and discharging rate. Conversely, the Online RBF controller demonstrates a reduced charge/discharge rate of the SC due to its enhanced adaptation and more refined regulation inputs, thereby signifying a more regulated and less stressed operation.

The distinctions in SoC between the PI controller and the Online RBF controller during the US06 and SC03 cycles are due to the different control strategies used to handle the battery and SC in these operational situations. Both controllers in the US06 cycle demonstrate consistent SoC patterns, which can be seen in Figures 9 & 10. Throughout the SC03 cycle, the PI controller indicates a substantial power loss, resulting in the battery's SoC dropping by almost 50% and the SC witnessing a 34% decrease, this can be seen in Figure 14 (a) & Figure 15 (a). The adaptability and ability to approximate complex, nonlinear systems are the primary factors behind the Online (RBF) controller's superior performance compared to the PI controller. This is illustrated in Figures 14 (b) & Figure 15 (b) by reduced losses of 0.35% for the battery and 1.2% for the SC. The difference illustrates how the choice of control system influences the energy management and performance of the HESS, showing the benefits of using the Online RBF controller in circumstances where reducing power losses and developing stability are essential.

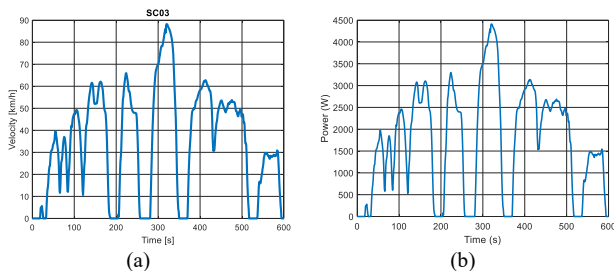


Figure 11. Representation of SC03 (a) Driving Cycle (b) Power Demand

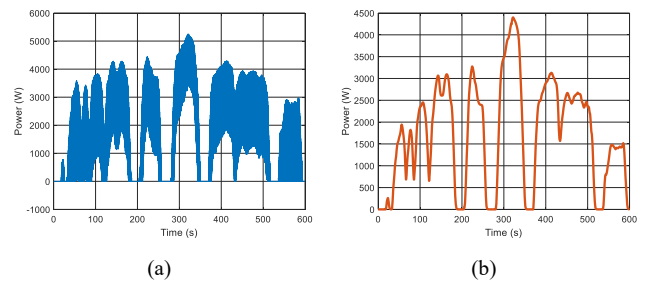


Figure 12. Representation of SC03 Battery Profile for (a) PI Controller (b) Online RBF Controller

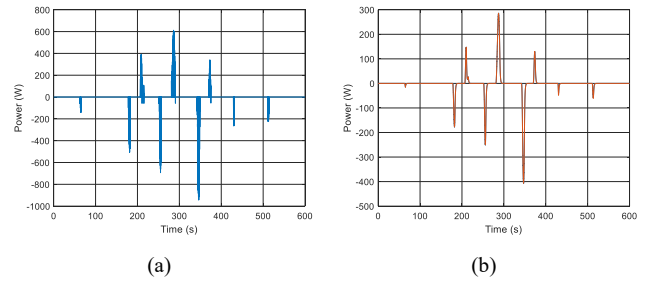


Figure 13. Representation of SC03 SC Profile for (a) PI Controller (b) Online RBF Controller

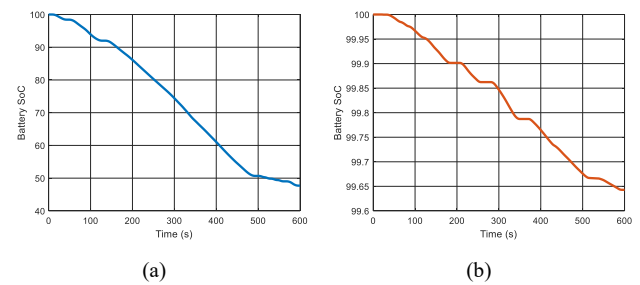


Figure 14. Representation of SC03 Battery SoC Profile for (a) PI Controller (b) Online RBF Controller

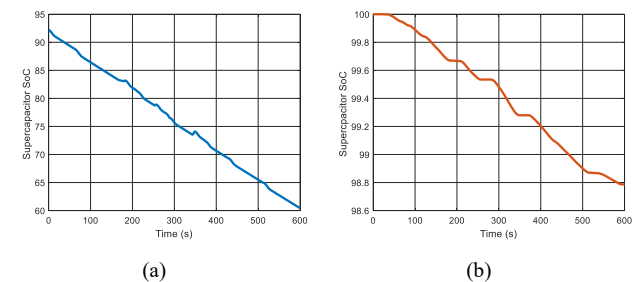


Figure 15. Representation of US06 SC SoC Profile for (a) PI Controller (b) Online RBF Controller

## V. CONCLUSIONS

Integrating SCs into the HESS effectively reduces stress on LIB's, enhancing the performance and lifespan of Electric Vehicles (EVs). The active architecture used effectively controls energy flow to enhance the system's efficiency. The comparison of PI and Online RBF controllers highlights the importance of choosing the appropriate control.

The PI controller, shown in Figures 7-10 and 12-15, demonstrates increased power fluctuations, particularly in the SC03 cycle. The battery has a roughly 50% drop in SoC and the supercapacitor witnesses a 34% fall, resulting in considerable energy losses. The Online RBF controller surpasses the PI controller by displaying a consistent power

profile, lower charge/discharge rates for the supercapacitor, and minimal losses of 0.35% for the battery and 1.2% for the supercapacitor. The results depicted in Figures 14b and 15b present a graphical illustration of the enhanced efficiency and stability attained with the Online RBF controller

The Online RBF controller's exceptional performance is mostly due to its versatility and ability to mimic complex, nonlinear systems. The findings demonstrate the significant influence of control techniques on energy management, underscoring the tangible advantages of selecting the Online RBF controller in real-world scenarios. The results provide important information on how to use HESS for EVs, highlighting the significant impact of control methods on improving energy efficiency, minimising power losses, and maximising system performance.

The study findings demonstrate that the Online RBF controller decreases power losses and maintains a controlled charge/discharge rate for the SC, strengthening both the effectiveness and stability of the HESS in EVs. This study enhances the overall comprehension of energy management systems in electric propulsion.

#### REFERENCES

- [1] Y. Ye, J. Zhang, and B. Xu, "A Fast Q-learning Energy Management Strategy for Battery/Supercapacitor Electric Vehicles Considering Energy Saving and Battery Aging," in *2021 International Conference on Electrical, Computer and Energy Technologies (ICECET)*, 2021, pp. 1–6.
- [2] A. Manthiram, "A reflection on lithium-ion battery cathode chemistry," *Nat. Commun.*, vol. 11, no. 1, p. 1550, 2020.
- [3] M. Adnane, B.-H. Nguyễn, A. Khoumsi, and J. P. F. Trovão, "Driving Mode Predictor-Based Real-Time Energy Management for Dual-Source Electric Vehicle," *IEEE Trans. Transp. Electrification*, vol. 7, no. 3, pp. 1173–1185, 2021.
- [4] M. Farrag, C. S. Lai, and M. Darwish, "Overview of Electric Vehicle Interconnected Subsystems," in *2022 57th International Universities Power Engineering Conference (UPEC)*, 2022, pp. 1–6.
- [5] L. Kouchachvili, W. Yaïci, and E. Entchev, "Hybrid battery/supercapacitor energy storage system for the electric vehicles," *J. Power*, vol. 374, pp. 237–248, 2018.
- [6] T. Sadeq, K. Chew, M. Ezra, Q. Abdullah, and O. Aydogdu, "Optimal Control Strategy to Maximize the Performance of Hybrid Energy Storage System for Electric Vehicle Considering Topography Information," *IEEE Access*, vol. 8, pp. 216994–217007, Jan. 2020.
- [7] M. B. Camara, H. Gualous, F. Gustin, A. Berthon, and B. Dakyo, "DC/DC Converter Design for Supercapacitor and Battery Power Management in Hybrid Vehicle Applications—Polynomial Control Strategy," *IEEE Trans. Ind. Electron.*, vol. 57, no. 2, pp. 587–597, 2010.
- [8] X. Wang, J. Tao, and R. Zhang, "Fuzzy energy management control for battery/ultra-capacitor hybrid electric vehicles," in *2016 Chinese Control and Decision Conference (CCDC)*, 2016, pp. 6207–6211.
- [9] P. Golchoubian and N. L. Azad, "Real-Time Nonlinear Model Predictive Control of a Battery–Supercapacitor Hybrid Energy Storage System in Electric Vehicles," *IEEE Trans. Veh. Technol.*, vol. 66, no. 11, pp. 9678–9688, 2017.
- [10] M. Sellali, S. Abdeddaim, A. Betka, A. Djerdir, S. Drid, and M. Tiar, "Fuzzy-Super twisting control implementation of battery/supercapacitor for electric vehicles," *ISA Trans.*, vol. 95, pp. 243–253, 2019.
- [11] X. Hu, Y. Li, C. Lv, and Y. Liu, "Optimal Energy Management and Sizing of a Dual Motor-Driven Electric Powertrain," *IEEE Trans. Power Electron.*, vol. 34, no. 8, pp. 7489–7501, 2019.
- [12] L. D. Seixas, H. G. Tosso, F. C. Corrêa, and J. J. Eckert, "Particle Swarm Optimization of a Fuzzy Controlled Hybrid Energy Storage System - HESS," in *2020 IEEE Vehicle Power and Propulsion Conference (VPPC)*, 2020, pp. 1–6.
- [13] G. Anbazhagan and C. Subramani, "A comprehensive review on energy management strategies of hybrid energy storage system for electric vehicles," *Int. J. Energy Res.*, vol. 41, Mar. 2017.
- [14] H. F. Gharibeh, L. M. Khiavi, M. Farrokhifar, A. Alahyari, and D. Pozo, "Power Management of Electric Vehicle Equipped with Battery and Supercapacitor Considering Irregular Terrain," in *2019 International Youth Conference on Radio Electronics, Electrical and Power Engineering (REEPE)*, 2019, pp. 1–5.
- [15] T. Sadeq, K. Chew, and M. Ezra, "Current Control of Battery-Supercapacitors System for Electric Vehicles based on Rule-Base Linear Quadratic Regulator," *Adv. Sci. Technol. Eng. Syst. J.*, vol. 6, pp. 57–65, Jan. 2021.
- [16] M. Farrag, C. S. Lai, and M. Darwish, *A Comparison of PI and RBF Brushless DC Motor Speed Control Methods*. 2023.